

MONITORING CHANGE DETECTION OF VEGETATION VULNERABILITY USING HOTSPOTS ANALYSIS

Basheer S. Jasim^{1,2*}, Oday Z. Jasim², Amjed N. AL-Hameedawi²

¹Technical Institute of Babylon, Al-Furat Al-Awsat Technical University, Iraq

²Civil Engineering Department, University of Technology - Iraq, Baghdad, Iraq

*Corresponding author: basheer.jasim@atu.edu.iq

(Received: 21 September 2023; Accepted: 30 January 2024; Published online: 15 July 2024)

ABSTRACT: Because of the ever-shifting nature of the weather conditions, which are made even more difficult by the dynamic relationship between the environment and the vegetation, one of the most important aspects is the vegetation. Landsat satellite imagery, TM sensor for 2002 and 2012, and OLI-TIRS sensor for 2022 were used for vegetation vulnerability. The Normalized Difference Vegetation Index (NDVI) method and hotspots analysis method were used for image classification, and the land cover map was obtained in three different years. The results of the analysis have shown that during 20 years, the extremely vulnerable zone has increased by 0.53%, the very vulnerable zone by 12.04%, and the moderately vulnerable zone has increased by 2.27% in terms of total area, also decreasing the non-significant zone by 5.74%, and the moderately safe zone decreased by 5.42%. The very safe zone decreased during this period by 2.94%. The extreme safe zone decreased by 0.73% in terms of total. Based on the assessment and validation of zone classification data, the overall accuracy value shows that the vegetation vulnerability accuracy for 2022 was equal to 90%. Also, the kappa coefficient for the classification vegetation vulnerability map was equal to 0.88. The research using Landsat data concluded that there had been a reduction in the amount of land covered by thick vegetation, which resulted in widespread drought conditions in some portions of the study region (Babylon Governorate). This research has shown that using satellite images and GIS spatial analysis is very effective in identifying and evaluating the trend of vegetation vulnerability in the Babylon Governorate. These data and techniques can be used for various analytical purposes.

ABSTRAK: Faktor perubahan cuaca yang mendadak, di mana hubungan dinamik antara alam sekitar dan tanaman menjadi lebih sukar, merupakan satu aspek penting bagi tumbuh-tumbuhan. Imej satelit Landsat, penerima TM 2002 dan 2012, dan penerima OLI-TIRS 2022 digunakan untuk tumbuh-tumbuhan yang terdedah. Kaedah Indeks Perubahan Ternormal Tumbuhan (NDVI) dan kaedah analisis kawasan khas digunakan bagi tujuan pengelasan imej, dan peta kawasan tanah berkaitan diperoleh dalam tiga tahun berbeza. Dapatan analisis menunjukkan selama 20 tahun, zon paling teruk terjejas telah bertambah sebanyak 0.53%, zon terjejas sebanyak 12.04%, zon sederhana terjejas bertambah kepada 2.27% berdasarkan total kawasan, juga pengurangan zon tidak penting 5.74%, zon sederhana selamat berkurang sebanyak 5.42%. Zon selamat telah berkurang selama tempoh ini sebanyak 2.94%. Zon paling selamat berkurang sebanyak 0.73% berdasarkan jumlah keseluruhan. Nilai ketepatan keseluruhan menunjukkan ketepatan tumbuh-tumbuhan terdedah pada 2022 bersamaan 90%, iaitu berdasarkan data klasifikasi zon pada ujian dan validasi. Juga, pekali kappa bagi klasifikasi peta tumbuh-tumbuhan terdedah bersamaan 0.88. Kesimpulan terhadap kajian menggunakan data Landsat ini adalah terdapat pengurangan pada bilangan tanah yang ditutupi oleh tumbuh-tumbuhan tebal, di mana menyebabkan keadaan kemarau yang berleluasa di

sebahagian kawasan yang dikaji (Babylon Governorate). Kajian ini menunjukkan dengan menggunakan imej satelit dan analisis ruang GIS, ianya sangat berkesan dalam mengenal pasti dan menganalisa perkembangan tumbuh-tumbuhan yang terdedah di Babylon Governorate. Data dan teknik ini boleh digunakan untuk pelbagai tujuan analisis.

KEYWORDS: *Vegetation vulnerability, NDVI, Vegetation Cover, Change detection, Hotspot analysis.*

1. INTRODUCTION

The change detection process requires using many temporal datasets to do a quantitative analysis of the phenomenon's impacts on the period [1][2]. Monitoring local, regional, and global resources and environments requires information on changes occurring on the world's surface [3][4]. The term "land cover" describes the various things that may be found on top of the Earth, both naturally and artificially [5]. The importance of land use lies in its relation with people's lives because it offers services directly in contact with people's needs [6][7]. The average temperature of the Earth's surface has increased, the average amount of precipitation has dropped, and the amount of land decertified has increased due to climate change and rising levels of human activity [8][9]. The remote sensing technique is crucial for creating maps showing land use and land cover from a procedure known as image classification [10]. The vegetation dynamics are essential in revealing how ecological systems respond to climate change [11]. Changes in vegetation may be caused by a wide variety of causes, including temperature and precipitation, ecological movement, grazing, and many more [12]. The environmental phenomenon known as "vegetation vulnerability" refers to how different driving factors work at varying degrees to cause the loss of vegetation. Natural fires, pests, illnesses, natural catastrophes, and even human conflict are all potential causes of vegetation loss. Agriculture is considered one of the most vulnerable sectors to drought compared to other sectors [13].

Several nations have extensively used remote sensing technology for effective environmental monitoring. In addition, many studies were conducted in various locations, including the United States, Europe, and others [14]. Multiple independent remote sensing indicators have been developed to evaluate the current status of the environment [15]. It is feasible to use conventional techniques for measuring the degree of appropriateness and susceptibility in any area, but doing so is very challenging and time-intensive [16]. In recent decades, geographic information systems (GIS) and satellite remote sensing (RS) technologies have gained substantial interest in suitability and vulnerability assessment. It has been proposed that these techniques are extremely effective [17].

Abdullah and Barua's. [18] A hybrid model was utilized to evaluate the model's accuracy in creating the hot spot map for 2021. The exact weight values have been used to forecast the hotspot map for 2026 and 2031, and the kappa statistics have been determined to be greater than 0.86 with 88.75 percent overall accuracy. The whole Nijhum Dwip region is split into seven zones using Gi* analysis, with the 90, 95, and 99% cold confidence levels being designated as moderately vulnerable zone (MVZ), very vulnerable zone (VVZ), and extremely susceptible zone (EVZ), respectively. However, the moderately safe zone (MSZ), very safe zone (VSZ), and extreme safe zone (ESZ), respectively, have been approved at the 99, 95, and 90 percent heat confidence levels. Additionally, it was considered that the remaining proportion of earth is an insignificant area (NSZ). The latter three kinds reflect safe places with the least to most vegetation clusters, whereas the first three indicate vulnerable areas with little or no vegetation. The NSZ is a barrier between the safe and vulnerable areas, which may change into other categories based on how well this boundary is maintained.

The hotspots of deforestation and forest fires in Andhra Pradesh, India, were identified by Reddy et al. [19] using historical patterns of deforestation (from 1975 to 1985 to 1995 to 2005 to 2014) and fire histories (2009-2014). The priority regions were selected as degradation and deforestation hotspots using a combination of deforestation danger metrics. In 2014, there were 25985 km² (16.2 percent of the entire geographical area) of forests in Andhra Pradesh. Between 1975 and 2014, a net deforested area of 2390 km² (8.4 percent) was calculated. Based on the prioritizing findings, deforestation and degradation hotspot-1 were identified in around 10.5 percent of existing forests due to severe ecological collapse.

According to research by Singh et al. [20], deforestation hotspots have been modeled as the forest regions with the highest densities of negative changes. The findings of the fragmentation analysis showed that core forests decreased during the research period. According to an examination of forest changes, between 1975 and 2015, the amount of land covered by forests decreased from 23749 km² (or 30.3 % of the state's geographical region) to 21145 km² (or 27 % of the state's geographical region). Assam's anticipated total forest area in 2030 is 20189 km² (25.7 %).

According to previous research findings, rainfall and temperature are the two most essential climate aspects contributing to vegetation changes. Increased human activities may further complicate the processes that influence vegetation changes due to climate change. NDVI is used to detect vegetation. A geographic statistical analysis converts each index pixel into points, indicating clustering based on a value in NDVI. The IDW method converts points into a surface that can be measured, and its areas are calculated. The problem is that no standard determines the division of NDVI, so the researcher chose a method that helps the division geographically and statistically. This study aims to explore vegetation vulnerability between 2002 and 2022 in the Babylon Governorate. The issues that need to be answered by the study are as follows: where are the sites of vegetation vulnerability change concentrated, how can places be identified in which the vulnerability of vegetation is most widespread, and where are the vegetation vulnerability and degradation hotspots?

2. THEORETICAL BACKGROUND

2.1. Image Preprocessing

The processing of images using satellite imagery is a significant difficulty. One of the most important duties in this field is recognizing individual objects inside a satellite image. Image restoration and rectification methods correct radiometric and geometric data distortions specific to certain sensors and platforms. These distortions might occur because of the sensor and platform interaction. Variations in scene lighting and viewing geometry, as well as changes in the conditions of the atmosphere, sensor noise, and responsiveness, may need radiometric adjustments [21]. These will differ based on the particular sensor and platform used to gather the data and the conditions present during the data acquisition [22].

2.1.1. Atmospheric Correction

Radiance data obtained by the sensor from the surface of the Earth are evaluated and corrected for distortions produced by the atmosphere and topography [23]. This correction aims to obtain surface reflectance values and restore the Earth's surface's physical characteristics by removing the atmosphere's effects from satellite images [24].

2.1.2 Radiometric Calibration

This procedure aims to convert the observed brightness into top-of-atmosphere reflectance. When constructing a multispectral or multitemporal mosaic, it is vital to follow this technique because it eliminates variations between images caused by variances in sensors, solar zenith angle, and distance between the Earth and the sun [25]. The following is a description of the process that must be followed to convert DN data to reflectance values. In the first step, the DN values are changed into radiance. Eq. (1) shows how the radiance value is converted to reflectance [26] where P is the TOA reflectance, $R\lambda$ is the spectral radiance, D is the Earth-sun distance in astronomical units from metadata, $E\lambda$ is the mean solar exoatmospheric irradiance (<https://landsat.usgs.gov>) and θ_s is the solar zenith angle from metadata.

$$P = \left[\frac{(\pi * R\lambda * d^2)}{(E\lambda * \cos\theta_s)} \right] \quad (1)$$

Temperature data is collected by satellite sensors like Landsat and recorded as a Digital number (DN) between 0 and 255. DNs from Landsat thermal bands are converted to spectral radiance using the image information and the following method to calculate brightness temperature [27] as shown in Eq. (2) where $R\lambda$ is the spectral radiance [$W/(m^2 \times sr \times \mu m)$], $Q.cal$ is the value of a pixel in a digital number, $Lmax$ is the spectral radiance (it is scaled to $Q.calmax$), $Lmin$ is the spectral radiance (it is scaled to $Q.calmin$), $Q.Calmax$ is the maximum calibrated value for a pixel and $Q.Calmin$ is the minimum calibrated value for a pixel.

$$R\lambda = \left[\frac{Lmax.\lambda - Lmin.\lambda}{Q.calmax - Q.calmin} \right] * [Q.cal - Q.calmin.] + Lmin.\lambda \quad (2)$$

2.2. Normalized Difference Vegetation Index

Computation of Normalized Difference Vegetation Index (NDVI) values for a Landsat image by the following formula [28]:

$$NDVI = \frac{(\rho.NIR - \rho.RE D)}{(\rho.NIR + \rho.RE D)} \quad (3)$$

where $\rho.RE D$ and $\rho.NIR$ are the red and near-infrared reflectance, respectively. NDVI values are within the range -1 to 1 , where negative values present loss of vegetation or contaminated vegetation, whereas positive values explain healthy and dense vegetation [29].

2.3. Hotspots Analysis

A "hotspot" is a region with a greater concentration of occurrences than expected from a random distribution of those events. This analytic tool identifies seven geographical patterns and the percentage of confidence levels for either warm or cold conditions (Gi Bin). The G_i^* analysis is a technique developed from studying point distributions or spatial groupings of points in a location [30]. The following equation is used for the calculation of Getis-Ord G_i^* according to the Eq. (4) (5) and (6) where, x_j is the attribute value for feature j , $w_{i,j}$ is the spatial weight between features i and j , n equals the total number of features, and the G_i^* is a z-score.

$$G_i^* = \frac{\sum_{j=1}^n w_{i,j} x_j - \bar{X} \sum_{j=1}^n w_{i,j}}{S \sqrt{\frac{n \sum_{j=1}^n w_{i,j}^2 - (\sum_{j=1}^n w_{i,j})^2}{n-1}}} \quad (4)$$

$$s = \sqrt{\frac{\sum_{j=1}^n x^2 j}{n}} - (\bar{X})^2 \tag{5}$$

$$\bar{X} = \frac{\sum_{j=1}^n x j}{n} \tag{6}$$

2.4. Inverse Distance Weighted

The Inverse Distance Weighted (IDW) approach is one of the most important geostatistical and mathematical interpolation methods [31]. The formula that is used to determine the value of the unknown variable $Z(S_0)$ at the position S_0 according to Eq. (7) and (8) where n is the number of the monitoring station, and $Z(S_i)$ is the value at each sampled place. S_i and W_i is the weight of S_i , which may be described as follows:

$$Z(S_0) = \sum_{i=1}^n W_i Z(S_i), \tag{7}$$

$$W_i = \frac{\frac{1}{d_i^k}}{(\sum_{i=1}^n \frac{1}{d_i^k})}, i = 1, 2, \dots, n \tag{8}$$

In this equation, d_i represents the horizontal distance that separates the interpolation points from those observed, and k is the power of the space.

2.5. Accuracy Assessment

Validation of the accuracy of the obtained categorized images using a kappa index and an error matrix [32]. The formula used to find kappa coefficients is:

$$\text{Kappa coefficient} = \frac{\sum_{i=1}^k n_{ii} - \sum_{i=1}^k n_{ii}(G_i C_i)}{n^2 - \sum_{i=1}^k n_{ii}(G_i C_i)} \tag{9}$$

where i is the number of the class, n is the total number of pixels that have been classified and will be compared with the actual data, n_{ii} represents the number of pixels that are part of the introductory data class i , that were classified as belonging to class i , C_i is the total number of pixels that correspond to class i that have been organized. G_i represents the total number of actual data pixels that belong to class i . Table 1 shows the accuracy rank for each kappa coefficient.

Table 1. Classification accuracy is based on the kappa value [33].

Kappa coefficient	Accuracy level
0.41–0.60	Moderate
0.61–0.80	High
≥0.80	Very high

2.6. Available Data and Methodology

Satellite data was used for this investigation. Landsat-5 TM images (for the years 2002 and 2012) and Landsat-8 OLI/TIRS images for the year 2022 were collected from the USGS (<https://earthexplorer.USGS.gov/>), details of which can be found in Table 2. These images and data were then used for the necessary geostatistical and geospatial analysis. This study used ENVI 5.3 and ArcGIS 10.8 software to process and analyze the datasets. Fig. 1 illustrates the methodology flowchart.

Table 2. Satellite information was used for this study.

No.	Satellite	Sensor	Path/Row	Date of Acquisition	Resolution	Product Type	Cloud Cover
1	Landsat-5	TM	168/38	22/10/2002	30 m	Landsat Collection 1 Level-1	0 %
2	Landsat-5	TM	168/37	22/10/2002			
3	Landsat-5	TM	168/38	18/10/2012			
4	Landsat-5	TM	168/37	18/10/2012			
5	Landsat-8	OLI/TIRS	168/38	13/10/2022			
6	Landsat-8	OLI/TIRS	168/37	13/10/2022			

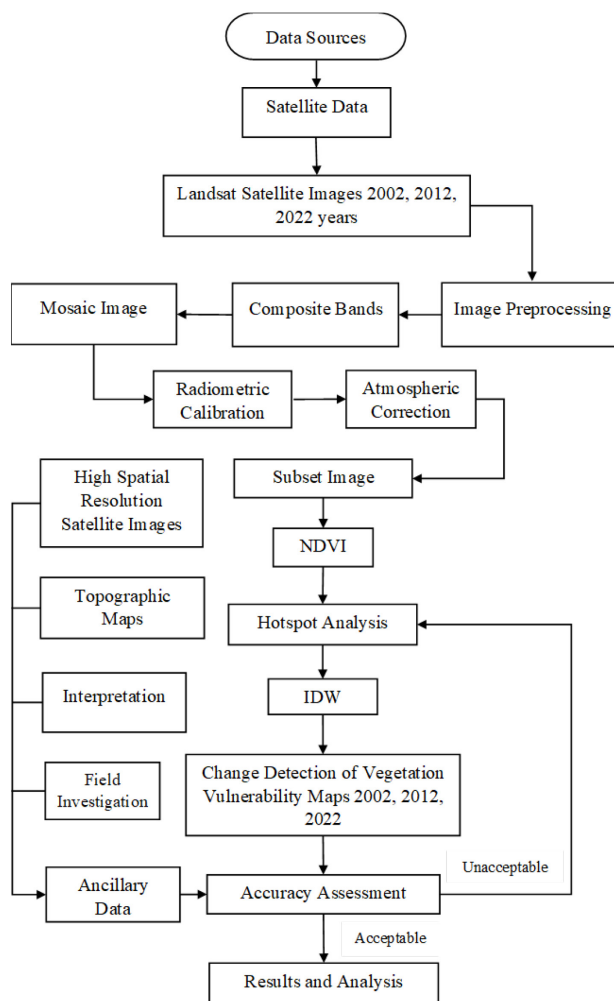


Figure 1. Flowchart for the general work.

3. STUDY AREA

The Babylon Governorate may be considered to be in the geographic middle of Iraq, located around 100 kilometers to the south of Baghdad, the capital of Iraq, between the longitudes of 44°2'43" East and 45°12'11" East, as well as the latitudes of 32°5'41" North and 33°7'36" North. Administratively, five major cities make up the Governorate as a whole [34]. These significant cities include Al-Hillah, Al-Qasim, Al-Hashimiyah, Al-Mahawil, and Al-Musayyab. According to calculations made using the program ArcGIS 10.8, the research region covers an area of about 5338 km². Fig. 2(a) and Fig. 2(b) show the study area map.

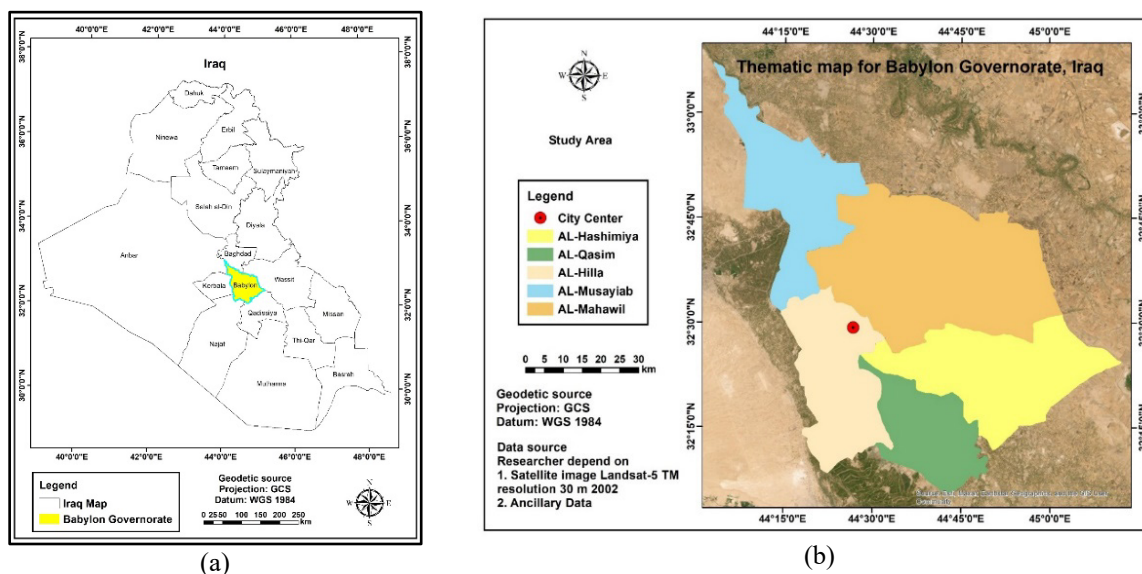


Figure 2. (a) The location of the study area in Iraq. (b) Geographical location map of Babylon Governorate.

4. RESULTS AND DISCUSSION

4.1 Change Detection

The production of digital maps is the first stage in building a database for all the measurements and information of a location [35][36]. To better understand the links and interactions between people and the natural environment, it is vital to collect information concerning changes in land cover. In this regard, remote sensing data has been one of the most important sources for studying the spatial and temporal changes in land cover in different regions. For processing and analysis, remote sensing multi-temporal datasets provide the possibility of mapping and identifying landscape changes and provide an effective step for sustainable local planning and management. In particular, by integrating RS and GIS techniques, it is possible to analyze and classify the changing patterns of land cover over a long period and, as a result, better understand the changes in the target range. This study adopts vegetation vulnerability classification in Table 3.

Table 3. Classification vegetation vulnerability classes following values proposed by [18].

No.	Hotspots	Zone
1	Cold spot 99% Confidence	Extremely vulnerable zone
2	Cold spot 95% Confidence	Very vulnerable zone
3	Cold spot 90% Confidence	Moderately vulnerable zone
4	Not Significant	Non-significant zone
5	Hot spot 90% Confidence	Moderately safe zone
6	Hot spot 95% Confidence	Very safe zone
7	Hot spot 99% Confidence	Extreme safe zone

This study computed the NDVI values using October Landsat images (TM and OLI/TIRS) for each year from 2002, 2012, and 2022. Fig. 3 represents the results of the NDVI index in the study area. Fig. 4 represents the results of the hotspot analysis based on the NDVI index in the study area. The calculated NDVI, hotspot change map, and IDW for the years 2002, 2012, and 2022 are presented in Fig. 5. Using the G_i^* method of analysis, the Babylon Governorate area is divided into seven different zones, where the 99%, 95%, and 90% cold confidence levels

have been categorized as extremely vulnerable, very vulnerable, and moderately vulnerable, respectively.

On the other hand, the 99%, 95%, and 90% hot confidence levels have been permitted as an extreme safe zone, very safe zone, and moderately safe zone, respectively. Besides, the middle category has been assumed to be a Non-significant zone. The first three kinds denote hazardous places with little to no vegetation, whereas the final three types denote safe areas with the fewest to the most plant clusters. It is possible for a non-significant zone, which serves as a buffer between a vulnerable zone and a safe zone, to transition into any of the other classifications depending on how well this balance is protected.

The information presented in Table 4 illustrates that the extremely vulnerable zone has increased from (13.47 to 41.85) km² in the study area between 2002 and 2022. Likewise, the very vulnerable zone also changed by approximately (733.77 to 1376.21) km² in the same period. Also, for the moderately vulnerable zone, there was an increase within the area it covered between the years (2002 and 2022), and it changed by approximately (1352.17 to 1473.23) km². At the same time, a decrease in four zones, the non-significant zone, moderately safe zone, very safe zone, and extreme safe zone, from the area it covered between (2002 to 2022) from (1334.31 to 1027.77) km² (1050.01 to 760.72) km², (638.73 to 481.61) km², and (214.60 to 175.66) km² respectively. According to the results of the extreme safe zone, there was an increase and then a decrease between the years (2002-2012) and (2012-2022) from (214.60 to 223.31) km², (223.31 to 175.66) km², respectively. Comparable with many researchers, such as [18][37][38].

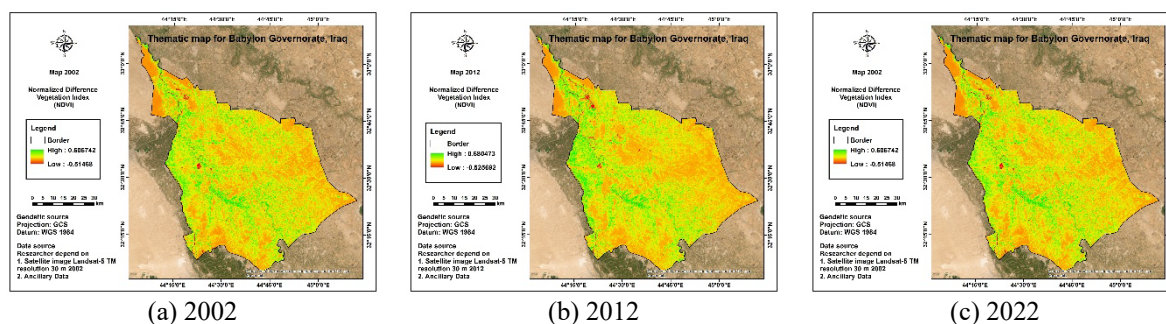


Figure 3. NDVI for years 2002, 2012, and 2022.

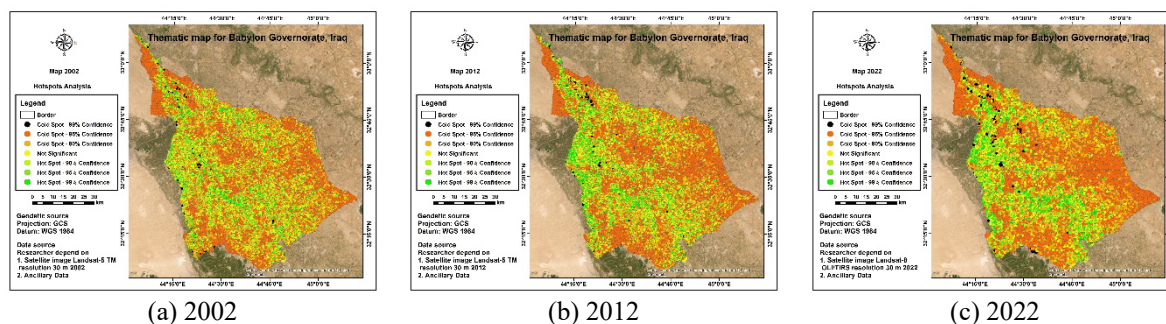


Figure 4. Hotspot analysis method for years 2002, 2012, and 2022.

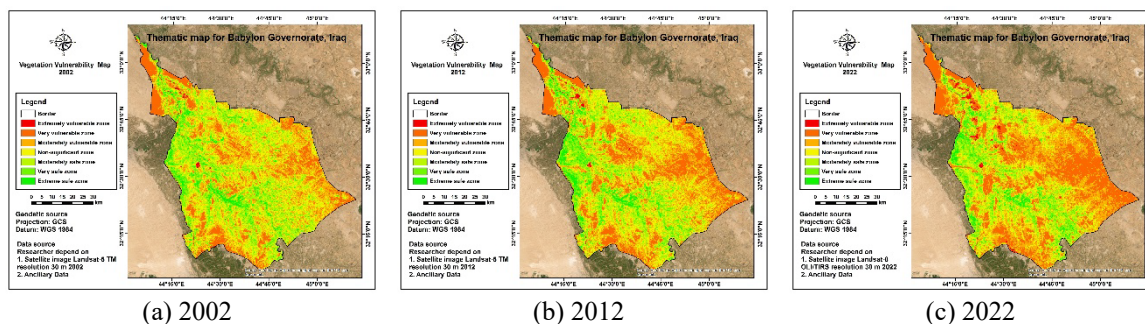


Figure 5. IDW method interpolation for years 2002, 2012, and 2022.

In Fig. 6, it can be seen that all three vulnerable zones increased between 2002 and 2022. In contrast, the three safe and non-significant zones decreased in 2002. This decrease was due to the lack of exploitation of water resources for agriculture, despite the increase in water between 2012 and 2022; according to the year 2002, the use of agricultural lands to be residential and the spread of residential slums. The exploitation of territory and natural resources is an essential component in the process of achieving sustainable development in the Governorate of Babylon. The destruction of green land can cause major harm to a region's environment and biodiversity. Again, alterations in the kinds of land present a significant challenge to regulators and managers, particularly in the Governorate of Babylon, where infrastructure construction is challenging and expensive. Therefore, those responsible for formulating policies and making plans must recognize these changes present a significant danger and act accordingly.

Table 4. Vegetation vulnerability changes in Babylon Governorate (2002-2022).

Zone	2002		2012		2022		Change trend
	Percentage (%)	Area (km ²)	Percentage (%)	Area (km ²)	Percentage (%)	Area (km ²)	
Extremely vulnerable zone	0.25	13.47	0.42	22.43	0.78	41.85	+ → +
Very vulnerable zone	13.75	733.77	18.32	977.75	25.79	1376.21	+ → +
Moderately vulnerable zone	25.34	1352.17	26.11	1393.26	27.60	1473.23	+ → +
Non-significant zone	25.00	1334.31	23.06	1230.80	19.26	1027.77	- → -
Moderately safe zone	19.67	1050.01	17.16	915.73	14.25	760.72	- → -
Very safe zone	11.97	638.73	10.75	573.78	9.02	481.61	- → -
Extreme safe zone	4.02	214.60	4.18	223.31	3.29	175.66	+ → -
Total	100.00	5337.05	100.00	5337.05	100.00	5337.06	

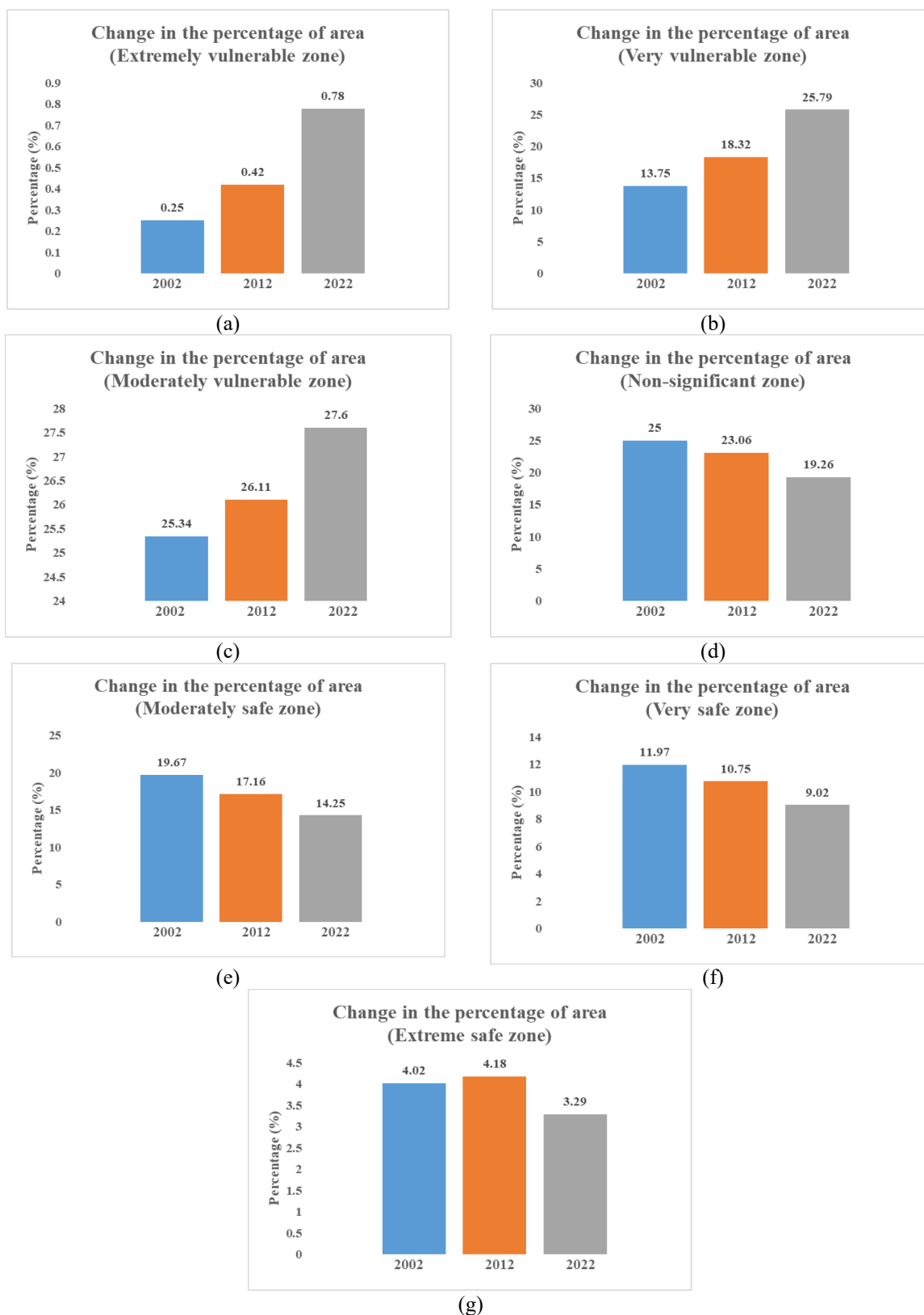


Fig. 6. Change in the percentage of the area (a to g) from 2002 to 2022.

Table 5 shows that the change occurred in the study area in the very vulnerable zone and the lowest change in the extreme safe zone between the years (2002-2012) and about 4.57% and 0.16%, respectively. In contrast, the change occurred in the study area in a very vulnerable zone and the least in an extremely vulnerable zone, about 7.47% and 0.36% between the years

(2012-2022), respectively. Finally, between the years (2002 and 2022), the change occurred in the study area in a very vulnerable zone, and the least change in an Extremely vulnerable zone was about 12.04% and 0.53%, respectively. The above analysis notes that the most changed zone is the very vulnerable zone. The area of gains and losses of each zone with vegetation vulnerability in Babylon Governorate for the years (2002-2012, 2012-2022, and 2002-2022). These changes may be linked directly to the interaction of physical and social variables such as the increase in population, lack of rain and water resources, climate change, population migration from the countryside to the city, and overgrazing. Fig. 7 elaborates on each category's gained and lost areas over each time interval.

Table 5. Gains and losses of each zone.

Zone	2002 - 2012		2012 - 2022		2002 - 2022	
	Percentage (%)	Area (km ²)	Percentage (%)	Area (km ²)	Percentage (%)	Area (km ²)
Extremely vulnerable zone	0.17	8.96	0.36	19.42	0.53	28.38
Very vulnerable zone	4.57	243.98	7.47	398.46	12.04	642.44
Moderately vulnerable zone	0.77	41.10	1.49	79.97	2.26	121.06
Non-significant zone	-1.94	-103.52	-3.8	-203.03	-5.74	-306.55
Moderately safe zone	-2.51	-134.28	-2.91	-155.01	-5.42	-289.28
Very safe zone	-1.22	-64.95	-1.73	-92.17	-2.95	-157.12
Extreme safe zone	0.16	8.71	-0.89	-47.64	-0.73	-38.93
Total	0.00	0.00	0.00	0.00	0.00	0.00

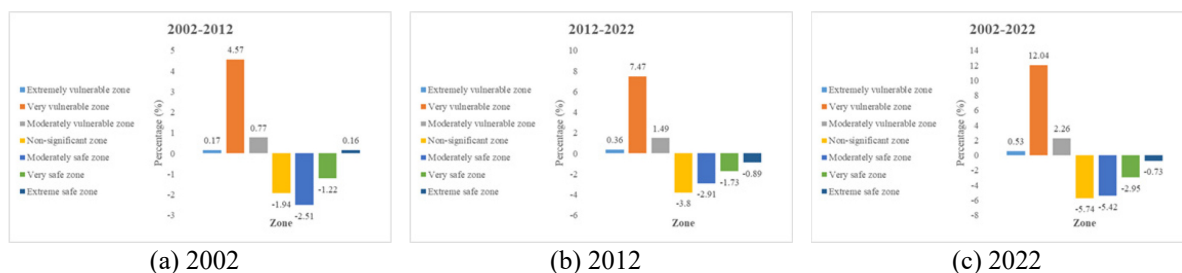


Fig. 7. Gains and losses in the percentage of the area (a to c) from 2002 to 2022.

The analysis of the results and achievements of the studies related to the identification of land changes has great value because it leads to the justification of the results and the necessity of citing the research findings, and on the other hand, it provides the ground for future research for other researchers. Collecting information about land cover changes is essential to better understanding the relationships and interactions between humans and the natural environment. In this regard, remote sensing data has been one of the most important data sources for studying the spatial and temporal changes of land cover in different regions. Remote sensing multi-temporal datasets for processing and analysis allows mapping and identifying landscape changes and provide an effective step for sustainable local planning and management. In particular, by integrating RS and GIS techniques, it is possible to analyze and classify the changing patterns of land cover over a long period and, as a result, better understand the changes in the target range. Today, it is well established that satellite remote sensing and GIS are the most common methods for quantifying, mapping, and detecting land use and land cover

change patterns because they have precise spatial analysis techniques and provide a suitable digital format for computer processing and repetitive data collection. Due to the capabilities of remote sensing and geographic information systems, scientists and researchers can detect large-scale changes in land use patterns with the knowledge they have acquired at the temporal and spatial levels, allowing politicians and regional authorities to make decisions.

4.2 Accuracy Assessment

The procedure was validated using reference data in 2022 and verified to be accurate. The methodology for the validation was based on the overall accuracy and kappa coefficient. A total of 280 validation points were surveyed based on an analysis of vegetation vulnerability maps and interpretation based on field observation and ancillary data such as topographic maps, high spatial resolution satellite images, and interpretation. According to the number of training samples analyzed to perform zone classification, the proportion of pixels classified in the correct or incorrect coverage class can be seen in Table 6, which indicates the acceptable error rate. On the other hand, the classification accuracy evaluation matrix was used to evaluate the overall classification accuracy, which is the main criterion for judging the results of the evaluations. Based on the assessment and validation of zone classification data, the overall accuracy value shows that the vegetation vulnerability accuracy for 2022 was equal to 90%. Also, the kappa coefficient for the classification map was 0.88. Therefore, according to the results of the accuracy evaluation, it can be said that the vegetation vulnerability classification process has been carried out with good accuracy and very high quality.

Table 6. Classification accuracy assessment matrix to vegetation vulnerability.

Zone	User's accuracy (%)	Producer's accuracy (%)
	2022	2022
Extremely vulnerable zone	100.00	77.50
Very vulnerable zone	89.19	82.50
Moderately vulnerable zone	81.25	97.50
Non-significant zone	82.93	85.00
Moderately safe zone	88.37	95.00
Very safe zone	100.00	97.50
Extreme safe zone	92.68	95.00
Overall accuracy = 90%		
Kappa coefficient = 0.88		

5. CONCLUSION

Analyzing the results and achievements of studies on identifying vegetation vulnerability is valuable because it justifies the results and the necessity of citing the research findings, while also providing a foundation for future research. The research results have shown that over the twenty years studied in Babylon Governorate, a significant portion of vegetation and crop cover has been lost and replaced by built-up lands. These findings can guide and inspire vegetation vulnerability studies and evaluation ideas in other regions. The region experienced a high percentage of vegetation drought from 2002 to 2022, highlighting the importance of monitoring vegetation changes. Remote sensing techniques have proven effective in observing vegetation vulnerability changes over substantial regions, and the hotspot analysis method has been

particularly useful in identifying areas of vulnerability. This research not only sheds light on past and present vegetation changes but also offers valuable methodologies for future studies in similar contexts.

REFERENCES

- [1] Kadhum ZM, Jasim BS, Obaid MK. (2020) Change detection in city of Hilla during period of 2007-2015 using Remote Sensing Techniques. *IOP Conf Ser Mater Sci Eng*. doi: 10.1088/1757-899X/737/1/012228
- [2] Al-Helaly MH, Alwan IA, Al-Hameedawi AN. (2021) Land covers monitoring for Bahar-Al-Najaf (Iraq) based on sentinel-2 imagery. *J Phys Conf Ser*. doi: 10.1088/1742-6596/1973/1/012189
- [3] Al-Helaly MH, Alwan IA, Al-Hameedawi AN. (2021) Assessing land cover for Bahar Al-Najaf using maximum likelihood (ML) and artificial neural network (ANN) algorithms. *J Phys Conf Ser*. doi: 10.1088/1742-6596/1973/1/012190
- [4] [Kadhum ZM, Jasim BS, Al-saedi ASJ. (2023) Improving the spectral and spatial resolution of satellite image using geomatics techniques Improving the Spectral and Spatial Resolution of Satellite Image Using Geomatics Techniques. 040011
- [5] Jasim O, Hasoon K, Sadiqe N. (2019) Mapping LCLU Using Python Scripting. *Engineering and Technology Journal*, 37(4A): 140–147. doi: 10.30684/etj.37.4a.5.
- [6] Al-Anbari R, Oday Zakariya, Mohammed ZT. (2016) Environmental and Urban Land Use Analysis by GIS in AL-Shaab of Baghdad as a case study. *Eng. &Tech.Journal* 34
- [7] Husein H, Jasim O, Mahmood S. (2018) Proposal of building a standard geodatabase for urban land use. *MATEC Web of Conferences*, 1621–5. doi: 10.1051/mateconf/201816203024.
- [8] Hasan SH, Al-Hameedawi ANM, Ismael HS. (2022) Supervised Classification Model Using Google Earth Engine Development Environment for Wasit Governorate. *IOP Conf Ser Earth Environ Sci*. doi: 10.1088/1755-1315/961/1/012051
- [9] Jabbar HK, Hamoodi MN, Al-Hameedawi AN. (2023) Urban heat islands: a review of contributing factors, effects and data. In: *IOP Conf. Ser. Earth Environ. Sci*. IOP Publishing. p 12038.
- [10] Al-Saedi ASJ, Kadhum ZM, Jasim BS. (2023) Land Use and Land Cover Analysis Using Geomatics Techniques in Amara City. *Ecol Eng*, 9161–169.
- [11] Muhammad R, Zhang W, Abbas Z et al. (2022) Spatiotemporal Change Analysis and Prediction of Future Land Use and Land Cover Changes Using QGIS MOLUSCE Plugin and Remote Sensing Big Data: A Case Study of Linyi, China. *Land*. doi: 10.3390/land11030419
- [12] Yu L, Wu Z, Du Z et al. (2021) Insights on the roles of climate and human activities to vegetation degradation and restoration in Beijing-Tianjin sandstorm source region. *Ecol Eng*. doi: 10.1016/j.ecoleng.2020.106105
- [13] Alwan I, Ziboon AR, Khalaf A. (2019) Monitoring of Agricultural Drought in the Middle Euphrates Area, Iraq Using Landsat Dataset. *Engineering and Technology Journal*, 37(7A): 222–226. doi: 10.30684/etj.37.7a.1.
- [14] Al-Hameedawi ANM, Abdulkhudhur R, Abdulkareem AO. (2022) Ground penetration radar based digital image processing for reinforcement corrosion in concrete. *Innovative Infrastructure Solutions*, 7(4): 241.
- [15] Sun CJ, Zhang WQ, Li XG, Sun JL. (2019) Evaluation of ecological effect of gully region of loess plateau based on remote sensing image. *Trans Chin Soc Agric Eng*, 35(12): 165–172.
- [16] Frazier PS, Page KJ. (2000) Water body detection and delineation with Landsat TM data. *Photogrammetric engineering and remote sensing*, 66(12): 1461–1468.
- [17] Khosravi K, Nohani E, Maroufinia E, Pourghasemi HR. (2016) A GIS-based flood susceptibility assessment and its mapping in Iran: a comparison between frequency ratio and weights-of-evidence bivariate statistical models with multi-criteria decision-making technique. *Natural hazards*, 83(2): 947–987.
- [18] Abdullah S, Barua D. (2022) Combining Geographical Information System (GIS) and machine learning to monitor and predict vegetation vulnerability: An Empirical Study on Nijhum Dwip,

- Bangladesh. *Ecological Engineering*, 178(January): 106577. doi: 10.1016/j.ecoleng.2022.106577.
- [19] Reddy CS, Manaswini G, Satish K V. et al. (2016) Conservation priorities of forest ecosystems: Evaluation of deforestation and degradation hotspots using geospatial techniques. *Ecological Engineering*, 91333–342. doi: 10.1016/j.ecoleng.2016.03.007.
- [20] Singh S, Reddy CS, Pasha SV et al. (2017) Modeling the spatial dynamics of deforestation and fragmentation using Multi-Layer Perceptron neural network and landscape fragmentation tool. *Ecological Engineering*, 99543–551. doi: 10.1016/j.ecoleng.2016.11.047.
- [21] Ziboon A, Albayati M, Dalhel F. (2022) Monitoring Soil Degradation in The Mesopotamian Plain Using GIS and Remote sensing Techniques. *Engineering and Technology Journal*, 40(5): 649–660. doi: 10.30684/etj.v40i5.2121.
- [22] Russ JC. (2006) *The image processing handbook*. CRC press.
- [23] Vargas-Cuentas N, Roman-Gonzalez A, Muñoz LA. (2017) Use of satellite images for droughts studying: The bolivian case.
- [24] Hadjimitsis DG, Papadavid G, Agapiou A et al. (2010) Atmospheric correction for satellite remotely sensed data intended for agricultural applications: impact on vegetation indices. *Natural Hazards and Earth System Sciences*, 10(1): 89–95.
- [25] Bruce CM, Hilbert DW. (2006) *Pre-processing methodology for application to Landsat TM/ETM+ imagery of the wet tropics*. Rainforest CRC Cairns, Australia.
- [26] Chittimalli SK. (2016) *Reflectance-based calibration and validation of the landsat satellite archive*. South Dakota State University.
- [27] Zaharaddeen I, Baba II, Zachariah A. (2016) Estimation of land surface temperature of Kaduna metropolis, Nigeria using Landsat images. *Science World Journal*, 11(3): 36–42.
- [28] Suresh S, Mani K. (2017) Application of remote sensing in understanding the relationship between NDVI and LST. *Int. J. Res. Eng. Technol.* 6
- [29] Jasim OZ. (2019) Using of machines learning in extraction of urban roads from DEM of LIDAR data: Case study at Baghdad expressways, Iraq. *Periodicals of Engineering and Natural Sciences*, 7(4): 1710–1721. doi: 10.21533/pen.v7i4.914.
- [30] Chakravorty S. (1995) Identifying crime clusters: The spatial principles. *Middle States Geographer*, 2853–58.
- [31] Yang W, Zhao Y, Wang D et al. (2020) Using principal components analysis and IDW interpolation to determine spatial and temporal changes of surface water quality of Xin'anjiang river in Huangshan, China. *International journal of environmental research and public health*, 17(8): 2942.
- [32] Jasim O, Hamed N, Abdulgabar T. (2018) Change detection and building spatial geodatabase for Iraqi marshes. *MATEC Web of Conferences*, 1623–6. doi: 10.1051/mateconf/201816203021.
- [33] Alwan IA, Aziz NA. (2021) An accuracy analysis comparison of supervised classification methods for mapping land cover using sentinel 2 images in the al-hawizeh marsh area, southern iraq. *Geomatics and Environmental Engineering*, 15(1): 5–21. doi: 10.7494/geom.2021.15.1.5.
- [34] Chabuk A, Al-Ansari N, Hussain HM et al. (2019) Landfill sites selection using MCDM and comparing method of change detection for Babylon Governorate, Iraq. *Environmental Science and Pollution Research*, 26(35): 35325–35339. doi: 10.1007/s11356-019-05064-7.
- [35] Jasim BS, Al-Bayati ZMK, Obaid MK. (2018) Accuracy of horizontal coordinates of cadastral maps after geographic regression and their modernization using gis techniques. *International Journal of Civil Engineering and Technology*, 9(11): 1395–1403.
- [36] Al-Hameedawi ANM. (2020) Comparison between Saaty's approach and Alonso and Lamata's approach in site selection process. *IOP Conf Ser Mater Sci Eng*. doi: 10.1088/1757-899X/737/1/012217
- [37] Alam KF, Ahamed T. (2022) Assessment of Land Use Land Cover Changes for Predicting Vulnerable Agricultural Lands in River Basins of Bangladesh Using Remote Sensing and a Fuzzy Expert System. *Remote Sensing*, 14(21): 5582.
- [38] Moradi E, Darabi H, Heydari Alamdarloo E et al. (2023) Vegetation vulnerability to hydrometeorological stresses in water-scarce areas using machine learning and remote sensing techniques. *Ecol Inform*. doi: 10.1016/j.ecoinf.2022.101838